APPLIED AND ENVIRONMENTAL MICROBIOLOGY, Dec. 1988, p. 3092–3100
0099-2240/88/123092-09$02.00/0

Vol. 54, No. 12

# Fast Kinetics of $Fe^{2+}$ Oxidation in Packed-Bed Reactors

SERGEI I. GRISHIN† AND OLLI H. TUOVINEN*
*Department of Microbiology, The Ohio State University, Columbus, Ohio 43210*

Received 29 June 1988/Accepted 7 September 1988

***Thiobacillus ferrooxidans*** **was used in fixed-film bioreactors to oxidize ferrous sulfate to ferric sulfate. Glass beads, ion-exchange resin, and activated-carbon particles were tested as support matrix materials. Activated carbon was tested in both a packed-bed bioreactor and a fluidized-bed bioreactor; the other matrix materials were used in packed-bed reactors. Activated carbon displayed the most suitable characteristics for use as a support matrix of *T. ferrooxidans* fixed-film formation. The reactors were operated within a pH range of 1.35 to 1.5, which effectively reduced the amount of ferric iron precipitation and eliminated diffusion control of mass transfer due to precipitation. The activated-carbon packed-bed reactor displayed the most favorable biomass holdup and kinetic performance related to ferrous sulfate oxidation. The fastest kinetic performance achieved with the activated-carbon packed-bed bioreactor was 78 g of $Fe^{2+}$ oxidized per liter per h (1,400 mmol of $Fe^{2+}$ oxidized per liter per h) at a true dilution rate of 40/h, which represents a hydraulic retention time of 1.5 min.**

*Thiobacillus ferrooxidans* has a unique ability to oxidize ferrous ion in sulfuric acid solutions, coupling the energy thus derived to support carbon dioxide fixation and growth. *T. ferrooxidans* is particularly suited for mineral leaching applications, because the bacterium can oxidize metal sulfides to acid-soluble sulfates. The oxidation of sulfide materials is also mediated by ferric ion, which in the reaction is chemically reduced to $Fe^{2+}$ and is reoxidized by *T. ferrooxidans*. Thus, during the leaching process, *T. ferrooxidans* also maintains a favorable $Fe^{3+}/Fe^{2+}$ ratio, which is reflected in the relatively high redox potential of the leach liquor.

Biological iron oxidation has been studied in several experimental systems with batch and continuous-flow modes of operation. Because of the interest in the kinetic aspects of the oxidation, attempts have been made to improve the ferrous iron oxidation rate by the use of various reactor designs employing biological contacting devices (8–11, 13). These have included bacteria in fixed-film applications to provide a large surface area for their attachment and to reduce the loss of biomass. Initial work with *T. ferrooxidans* was primarily concerned with the development of rotating biological contactors. More recent efforts have addressed other fixed-film approaches, which essentially involve various configurations of packed-bed and fluidized-bed reactors with inert carrier matrix materials. In the present work, various carrier matrix materials were evaluated with respect to the kinetics of ferrous iron oxidation in packed-bed reactor systems. As a reference, a fluidized-bed reactor was also tested with one type of matrix material. A novel feature in the present study was the use of a low pH to provide more space for the bacterial sorption by elimination of Fe(III) precipitation.

## MATERIALS AND METHODS

The following equations were used to obtain the data presented in this paper: $C = 100\ (S_{in} - S_{out})/S_{in}$; $D = F/V_r$; $D_t = F/V_l$; $K_{1,2} = \Delta Pr/\Delta t$; $Pr = DP = D\ (S_{in} - S_{out})\ Y_{P/S}$ (where $Y_{P/S} = 1$); $q = R/X_l$; $R = D_t\ (S_{in} - S_{out})$; $\tau = 1/D_t$; $V_t = V_a + V_l + V_m + V_f$. The definitions and dimensions of the variables are presented in Table 1.

A packed-bed reactor design was based on a glass column (16 by 320 mm) with inlets for fresh medium and air at the bottom. The total reactor working volume was 50 ml. The outlet for effluent and exhaust air was at the top of the column. The reactors were aerated at 120 ml/min, and the flow rates for fresh media were regulated with peristaltic pumps. As a reference system, a fluidized-bed reactor was tested with activated carbon as a support matrix. The reactor was conical (maximum dimensions, 70 by 160 mm) and had a total operating volume of 150 ml. The reactors were maintained at 23°C.

Activated carbon, glass beads, and ion-exchange resin were tested as biomass-support matrices (Table 2). The size fraction was defined by the manufacturer of each matrix material. A spherical shape was assumed for each particle, and the arithmetic mean of each size fraction was used for surface area calculations. The total and liquid volumes of the reactors were experimentally determined.

Two media, each containing 120 mM ferrous sulfate, were tested in the course of the work: (i) a mineral salts solution containing 2.3 mM $K_2HPO_4$, 1.6 mM $MgSO_4$, and 3.0 mM $(NH_4)_2SO_4$, and (ii) tap water. According to water quality monitoring by the Columbus Division of Water, composited tap water samples averaged (per liter) 10 mg of Mg, 27 mg of Ca, 1.50 mg of nitrate, and 0.34 mg of total phosphate. Both media were acidified to an initial pH of 1.35 with sulfuric acid. The test bacterium was *T. ferrooxidans* TFI-35, which had been routinely maintained with ferrous sulfate in liquid media at pH 1.5. Ferrous sulfate oxidation was monitored by $KMnO_4$ titration of the residual ferrous iron in effluent samples.

For protein determination, bacteria were concentrated by centrifugation at 4,350 × *g* for 30 min and then washed four times with 0.1 N sulfuric acid. The samples were digested in 1 N NaOH for 10 min at 90°C. The protein measurement was performed by the Lowry method using bovine serum albumin (Sigma Chemical Co.) as a reference. Biomass attached on support carrier matrices in the reactors was also quantitated by protein determination. Because of the sensitivity of the system to physical disturbance upon sampling and the uneven distribution of the attached cells, the biomass associated with particle surfaces was analyzed only at the

* Corresponding author.
† Present address: Moscow Steel and Alloys Institute, 117465 Moscow, USSR.

TABLE 1. Variables used in this study

| Variable | Definition | Dimensions |
|---|---|---|
| $A$ | Surface area | $cm^2$ |
| $C$ | $Fe^{2+}$ conversion | % |
| $D$ | Dilution rate (vs. total reactor vol) | 1/h |
| $D_t$ | True dilution rate | 1/h |
| $F$ | Flow rate of medium | ml/h |
| $K_{1,2}$ | Productivity decline coefficient | mmol/liter per h per day |
| $P$ | Product ($Fe^{3+}$) concn | mmol/liter |
| $Pr$ | Reactor productivity | mmol per liter per h and g per liter per h |
| $q$ | Oxidation quotient | mmol of $Fe^{2+}$ oxidized per mg of protein per h |
| $R$ | $FeSO_4$ oxidation rate | mmol per liter per h and g per liter per h |
| $S_{in}$ | $Fe^{2+}$ influent concn | mmol/liter |
| $S_{out}$ | $Fe^{2+}$ effluent concn | mmol/liter |
| $\tau$ | Retention time | min |
| $t$ | Time | days |
| $V_a$ | Total vol of air bubbles within reactor | ml |
| $V_f$ | Total fixed film vol | ml |
| $V_l$ | Interstitial liquid vol | ml |
| $V_m$ | Total matrix vol | ml |
| $V_t$ | Total vol of reactor | ml |
| $X_l$ | Biomass concn per interstitial liquid vol of reactor | mg of protein/ml |
| $Y_{P/S}$ | Yield of product from substrate | |

termination of each bioreactor. The biomass on the support matrix materials was fractionated as follows. Loosely bound biomass was removed by washing and stripping the bead samples with 0.1 N $H_2SO_4$, and the remaining cell fraction on the beads was termed tightly bound protein. A part of each matrix sample material was also used for analysis of the total protein in the biofilm, which was determined without sample pretreatment by washing and stripping. In all cases, the difference between the total biomass and the fractionated biomass was <5%.

## RESULTS

**Operation of the packed-bed reactors.** Several experimental runs were carried out to determine the influence of carrier matrix materials and surface area on the bacterial film formation and rate of ferrous iron oxidation. Each bioreactor was operated as an independent unit and was started with a 10% (vol/vol) inoculum of a spent, iron-grown culture of *T. ferrooxidans*. In all experiments, the bacterial fixed film was initially formed on the carrier matrix during batch-mode operation of the reactors. Once 95% conversion of ferrous iron was achieved, a continuous-flow mode of operation was initiated. The continuous-flow systems were operated without any subsequent, additional inoculation for 90 to 120 days until the experiments were terminated. The solution flow rates were controlled with peristaltic pumps and changed stepwise during the experiments.

Steady-state conditions were used at each flow rate for estimating the kinetics of ferrous sulfate oxidation. After a change in the flow rate, steady-state conditions were achieved when no further change occurred in the iron oxidation rate. The time required to achieve steady-state conditions at each flow rate varied depending on the flow rate and the carrier matrix. In packed-bed reactors with activated-carbon or resin particles as the carrier matrix and operated at dilution rates below 2/h, the steady-state conditions were reached within 12 h of the change of the flow rate. Similarly, packed-bead reactors with glass beads reached steady-state conditions within 12 h when operated at dilution rates below 0.5/h. At high dilution rates of 2/h to 4/h, packed-bed reactors with activated carbon took up to 6 to 8 days before the steady-state conditions were established.

The operation of the reactors was disrupted several times for 8 to 12 h because of various unforeseen technical problems. In each case, when the operation was resumed, the bacterial oxidation of ferrous iron ensued without delay.

**Productivity in the packed-bed reactors.** The productivity of the bioreactors can be used to express the rate of ferric iron production, which was estimated on the basis of the dilution rate and the total working volume. All packed-bed reactors displayed a similar response in terms of the productivity and dilution rate (Fig. 1 to 4). Three phases could be distinguished in these responses. The productivity increased at low dilution rates, leveled off at intermediate dilution rates, and declined at high dilution rates. This three-phase response is a typical feature in general for immobilized cell systems. The packed-bed reactors with resin particles and activated carbon (Fig. 3 and 4, respectively) displayed the most characteristic and sharpest phase responses. At dilution rates below 2/h in these reactors, virtually all ferrous iron was oxidized. Under these conditions, the oxidation rate only depended on the dilution rate: $R = S_{in} \times D$. The plateau of productivity in Fig. 1 to 4 represents an area

TABLE 2. Physical characteristics of test reactors

| Reactor no. | Text matrix | Source | Reactor type | Size fraction (μm) | Total matrix surface in reactor ($cm^2$) | Total reactor vol (ml) | Total vol of interstitial liquid per reactor (ml) | Total reactor working vol (ml) |
|---|---|---|---|---|---|---|---|---|
| 1 | Glass beads | Sigma | Packed bed | 710–1,180 | 2,000 | 65 | 20 | 50 |
| 2 | Glass beads | Sigma | Packed bed | 425–600 | 3,700 | 64 | 16 to 20[a] | 50 |
| 3 | Resin beads (Amberlite IR-45) | Mallinkrodt, Inc. | Packed bed | 400–1,100 | 2,500 | 65 | 17 | 50 |
| 4 | Activated carbon | Union Carbide Corp. | Packed bed | 701–841 | 2,500 | 65 | 10 | 50 |
| 5 | Activated carbon | Union Carbide | Fluidized bed | 212–300 | 2,500 | 250 | 140 | 150 |
| | | | | | 5,000 | | 130 | 150 |
| | | | | | 7,500 | | 120 | 150 |

[a] Volume varied depending on the flow rate.

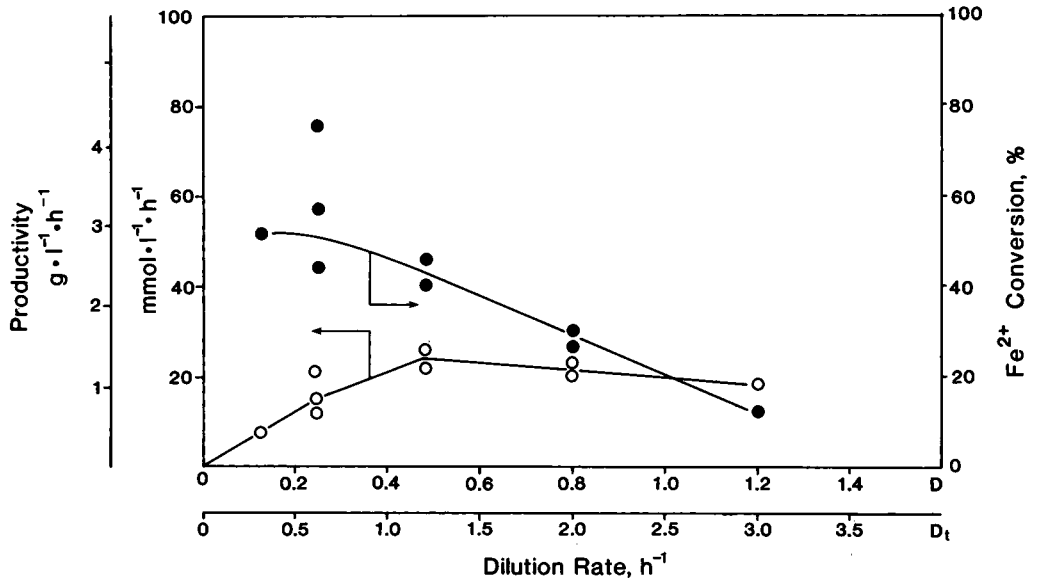


FIG. 1. Ferric iron productivity (○) and ferrous iron conversion (●) in glass-bead packed-bed reactor no. 1 (710- to 1,180-μm-size beads) at various dilution rates.

which was dependent on biomass concentration in the fixed film but was independent of the dilution rate. With all carrier matrix materials, a washout effect occurred at high dilution rates which resulted in decreased productivity. The critical dilution rate, at which the washout effect occurred, depended on the type of carrier matrix material. For glass beads, the washout occurred at dilution rates of >0.6/h for reactor 1 (710- to 1,180-μm-size fraction) and 1.2/h for reactor 2 (425- to 600-μm-size fraction). The critical dilution rates for activated-carbon and ion-exchange resin bioreactors were >6/h and >2/h, respectively.

The activated-carbon bioreactor displayed a multiple response of productivity at dilution rates between 2/h and 4/h. The dependency between the productivity and the dilution rate was related to the direction of the flow rate change, i.e., whether the flow rate was increased or decreased in this range. The direction of the change is indicated with arrows in Fig. 4. The peak response in productivity was reached upon increased flow rate, but a further increase counteracted the peak response. In the plateau range, which typically resulted when a high flow rate was decreased, the productivity increased if the bioreactor was subsequently given 5 to 10 days to reach a steady state (Fig. 4). This improved productivity after the flow rate was decreased is indicated by arrow J in Fig. 4.

In each bioreactor, a plateau and a declining phase of

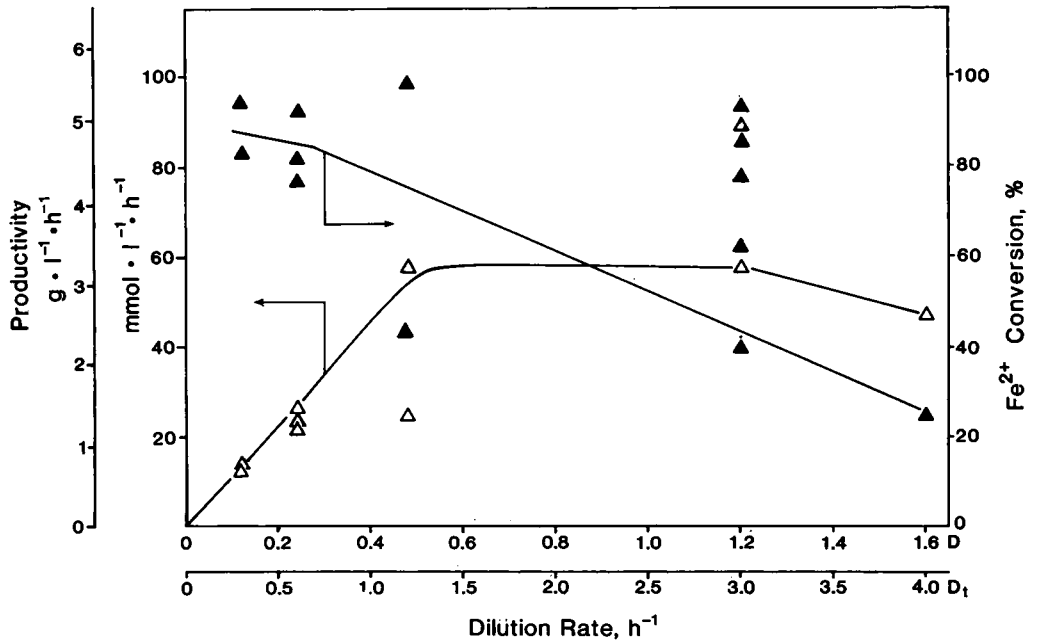


FIG. 2. Ferric iron productivity (△) and ferrous iron conversion (▲) in glass-bead packed-bed reactor no. 2 (425- to 600-μm-size beads) at various dilution rates.

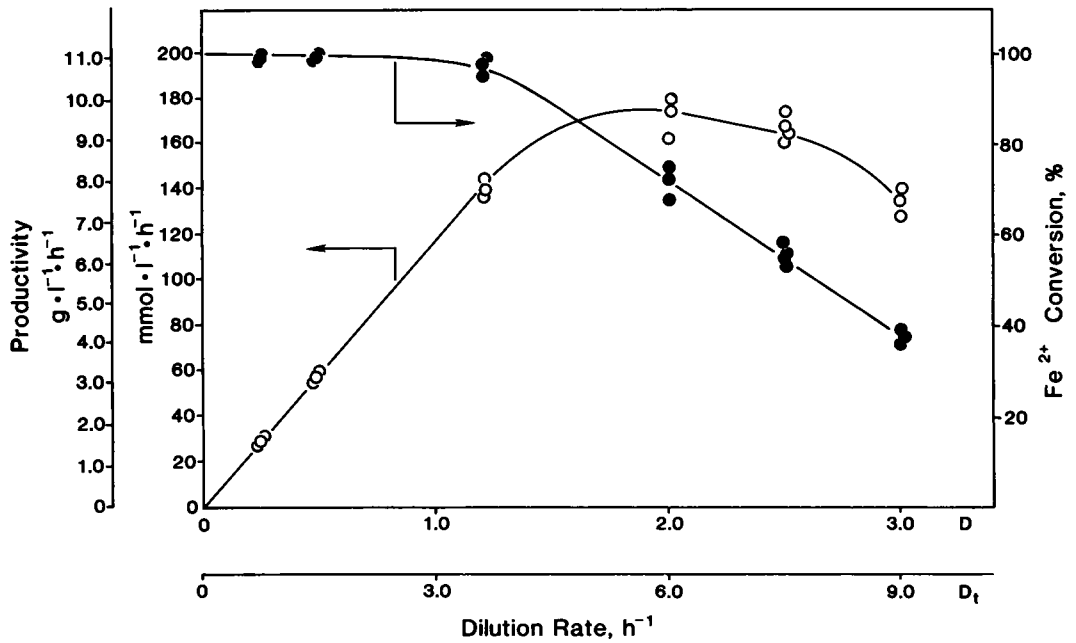


FIG. 3. Ferric iron productivity (○) and ferrous iron conversion (●) in ion-exchange resin packed-bed reactor no. 3 (400- to 1,100-μm-size beads) at various dilution rates.

productivity could be discerned; these were associated with descending values of ferrous iron conversion (Fig. 1 to 3 and 5). In order to estimate the kinetics of ferrous iron oxidation by the fixed-film biomass, the true dilution rate ($D_t$) was used as a parameter for calculations. The $D_t$ is the reciprocal of the retention time of the solution in the bioreactor and was therefore calculated on the basis of the interstitial liquid volume in each packed-bed reactor. The highest $D_t$ values were obtained with the packed-bed reactor in which activated carbon was used as a carrier matrix material. This reactor could be operated at $D_t$ values as high as 40/h (i.e., 1.5-min retention time), with corresponding productivity values of 144 mmol of $Fe^{2+}$ oxidized per liter per h (8 g/liter per h). The highest productivity value was 280 mmol of $FeSO_4$ oxidized per liter per h in the activated carbon packed-bed reactor and 25 and 58 mmol of $FeSO_4$ oxidized per liter per h in reactors 1 (glass beads; 710- to 1,180-μm-size fraction) and 2 (glass beads; 425- to 600-μm-size fraction), respectively. The packed-bed bioreactor operated with ion-exchange resin particles had productivity values in the intermediate range between those of the glass-bead and activated-carbon systems, with a maximum of 175 mmol of $FeSO_4$ oxidized per liter per h.

**Fluidized-bed reactor.** A fluidized-bed reactor was also tested with activated carbon as the support matrix to provide reference data for the evaluation of the packed-bed reactor approach. Activated carbon was chosen for the fluidized-bed reactor because it appeared to have superior properties among the test matrix materials in terms of productivity estimates in packed-bed reactors. A smaller-size-fraction sample of activated carbon was used in these experiments compared with packed-bed experiments. In some experiments, the total surface area was standardized to an equal value in the two different reactor designs. Conditions were also used under which the total surface area in the fluidized-bed bioreactor exceeded that in the packed-bed bioreactor by factors of 2 and 3.

The productivity achieved with the fluidized-bed system was at least 10 times lower than that achieved with the packed-bed system. It had a constant value of 16 mmol of $Fe^{2+}$ oxidized per liter per h (0.9 g/liter per h) at $D$ values in the range of 0.1/h to 0.4/h when the surface area was standardized to 16 $cm^2$/ml (6.5% pulp density) in the reactor (Fig. 6). The productivity in this test system was dependent on the quantity of the carrier matrix material used in the reactor and displayed a linear increase of up to 28 mmol of

TABLE 3. Biomass in the test reactors

| Reactor no. | Mg of protein per reactor | | | Mg of protein per ml of reactor vol | | | μg of protein per $cm^2$ of carrier matrix surface | | | Protein sorption (mg) per ml of interstitial liquid | | | μg of protein per ml of effluent[b] |
|---|---|---|---|---|---|---|---|---|---|---|---|---|---|
| | Loosely bound | Tightly bound | Total | Loosely bound | Tightly bound | Total | Loosely bound | Tightly bound | Total | Loosely bound | Tightly bound | Total | |
| 1 | 3.4 | 1.5 | 5.1 | 0.068 | 0.032 | 0.1 | 1.75 | 0.75 | 2.5 | 0.18 | 0.07 | 0.25 | 3-15 |
| 2 | 5.5 | 2.7 | 7.3 | 0.1 | 0.05 | 0.15 | 1.45 | 0.65 | 2.1 | 0.32 | 0.16 | 0.48 | 3-15 |
| 3 | 73 | 39 | 112 | 1.4 | 0.8 | 2.2 | 29.2 | 15.6 | 44.8 | 4.3 | 2.3 | 6.6 | 3-20 |
| 4 | 238 | 110 | 320 | 4.7 | 2.2 | 6.4 | 95 | 44 | 128 | 24 | 11 | 32 | 3-20 |
| 5 | | 15 | 17[a] | | | 0.11 | | | 3 | | | 0.015 | 15 |

[a] Total protein in the fluidized bed reactor consisted of tightly bound cells plus freely suspended cells.
[b] Protein concentrations in the effluent fluctuated with no apparent dependence on either the flow rate or length of operation.

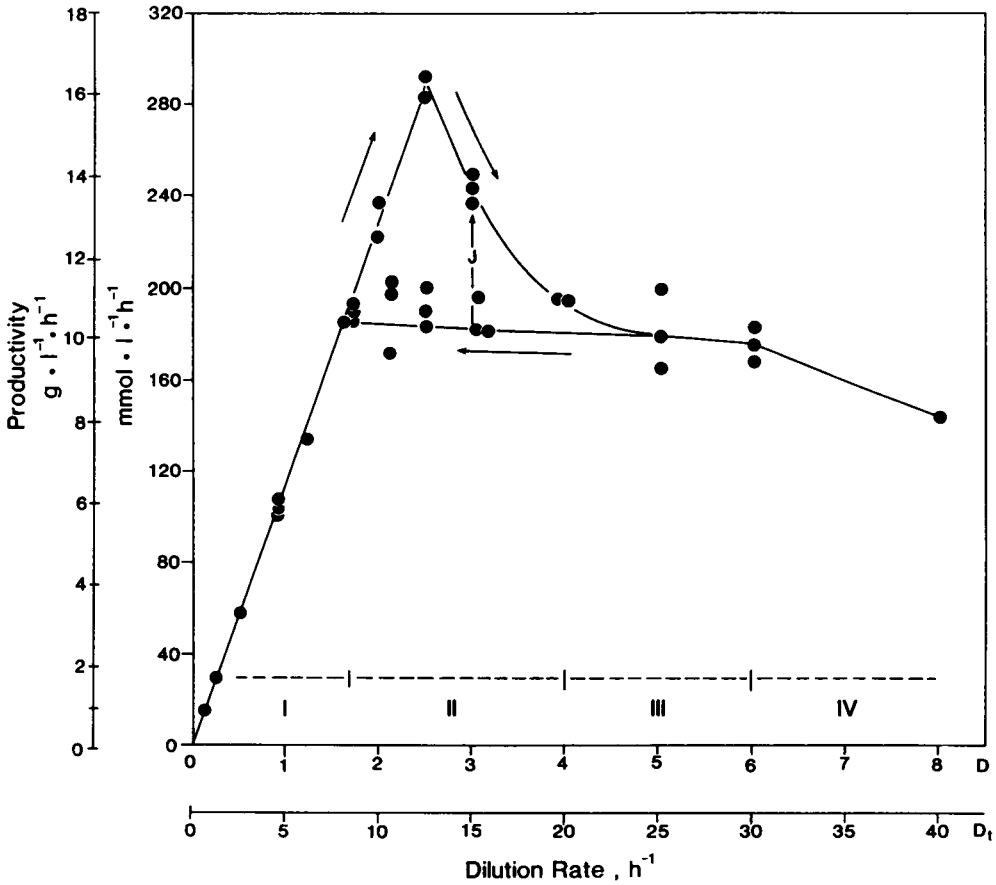


FIG. 4. Ferric iron productivity in activated-carbon packed-bed reactor no. 4 (701- to 841-μm-size beads) at various dilution rates. The unlabeled arrows indicate the direction of the dilution rate change; arrow J is explained in Results. The different phases labeled I through IV are discussed in the text.

$Fe^{2+}$ oxidized per liter per h at $D$ = 0.4/h when the pulp density of activated carbon was increased in the range of 66 to 200 g/liter (Fig. 7).

**Biomass concentration.** The amount of biomass in the reactors was determined at the termination of the experiments. The biomass values thus analyzed coincided with the testing of the reactors close to the critical $D$ values. The activated-carbon packed-bed reactor had the highest level of biomass (Table 3), amounting to 32 mg of protein per ml of interstitial liquid or 128 μg of protein per $cm^2$ of matrix surface. The ability of the glass beads to retain biomass was about 50 times less. The two glass-bead reactors contained more or less the same amount of biomass per unit surface area (2.5 and 2.1 μg of protein per $cm^2$ of glass bead surface in reactors 1 and 2, respectively). However, the total amount of biomass was about 1.5 times higher in reactor 2, in which the glass beads had a smaller particle size and, therefore, a higher surface area than the beads in reactor 1 did (Table 3). In the fluidized-bed reactor containing activated-carbon particles as the carrier matrix, the biomass sorption per unit surface area was similar to that found with glass beads (Table 3). The fluidized-bed reactor had ca. 40 times less biomass than did the activated-carbon packed-bed reactor (Table 3). The interior surface of the reactor wall had a surface area of 160 $cm^2$. Depending on the test matrix material, this surface area represents 4 to 8% of the total available surface per reactor. The interior wall surface has been excluded in biomass sorption and holdup calculations.

The ratio of loosely bound biomass to tightly bound biomass in the packed-bed reactors was approximately 1:2 in each case. This proportion was estimated only on the basis of the sample pretreatment (stripping) procedure used for protein determination. In the packed-bed reactors, the effluent biomass concentrations fluctuated within each flow rate regime and appeared to have no discernible relationship with the prevailing flow rate.

**Biomass holdup.** The maximum biomass holdup (the amount of biomass retained in each bioreactor) occurred in the activated-carbon packed-bed bioreactor. There were major differences in the biomass holdup due to the different types of matrix materials. Glass beads (425- to 600-μm-size fraction) had a surface area which was 1.5 times larger than that of the activated carbon, but the biomass in the glass-bead packed-bed reactor was about 50 times less than that in the activated-carbon packed-bed reactor. Because of the importance of this parameter in performance assessment and in the prediction of reactor capability, the interstitial volumes and actual values of biomass hold-up were estimated for each bioreactor. These estimates are presented in Table 4, and they single out the activated-carbon packed-bed reactor as the most promising type of the reactors tested. The estimation of the potential biomass holdup was based on the calculation of the void volume in a bioreactor filled with spherical particles and on the respective, constant volume of liquid and air bubbles. The estimation of the actual biomass holdup was based on protein determination of samples

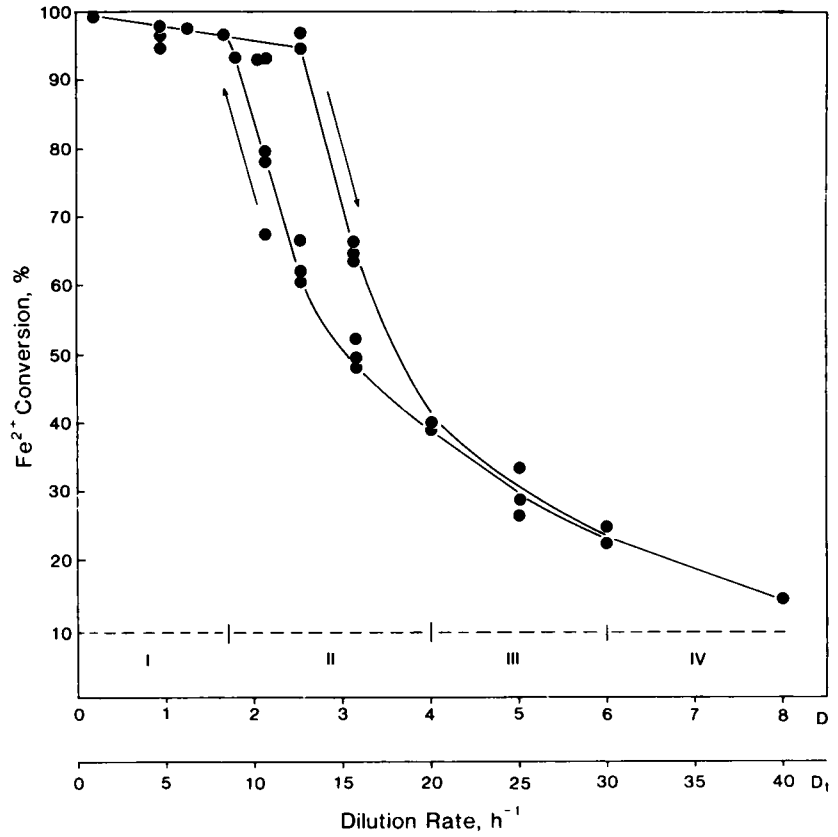


FIG. 5. Ferrous iron conversion in the activated-carbon packed-bed reactor no. 4 (701- to 841-μm-size particles) at various dilution rates. The arrows indicate the direction of the dilution rate change. The different phases labeled I through IV are discussed in the text.

removed from the bioreactors. The biomass value presented for a monolayer film of bacteria that could exist in the packed-bed activated-carbon reactor at a given biomass value of 320 mg of protein per reactor volume was based on the approximation that the surface occupied by a single cell (average size, 0.35 by 0.95 μm) was 0.33 $\mu m^2$. The following biomass conversions were made to derive the biomass holdup estimates: protein constitutes 60% of the dry weight; dry weight equals 20% of the wet weight; specific density of the biomass is 1.05; and 1 mg of protein equals $10^{10}$ cells. The maximum observed biomass holdup was 27% of the potential value for the activated-carbon packed-bed reactor (Table 4). It should be noted that the observed and potential values for biomass holdup cannot approach an equal level because of the inherent problem of diffusion under such conditions. The data in Table 4 include an estimate of 4.2 monolayers of bacterial cells on the activated-carbon particles in the packed-bed reactor.

While the monolayer estimates highlight the differences between the test carrier matrix materials, they are only relative values and should be used with caution. Parallel examination of the packed carrier matrix materials by scan-

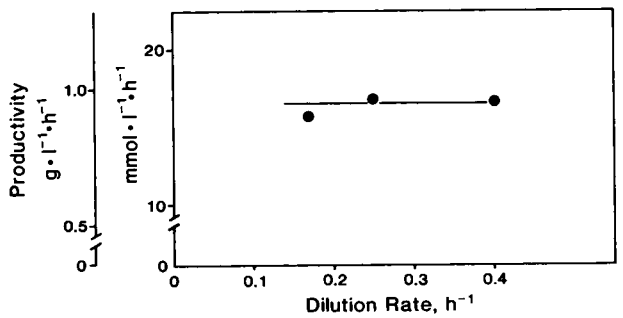


FIG. 6. Ferric iron productivity in the activated-carbon fluidized-bed bioreactor no. 5 (212- to 300-μm-size particles) at various dilution rates. The pulp density was 6.5% in these experiments.

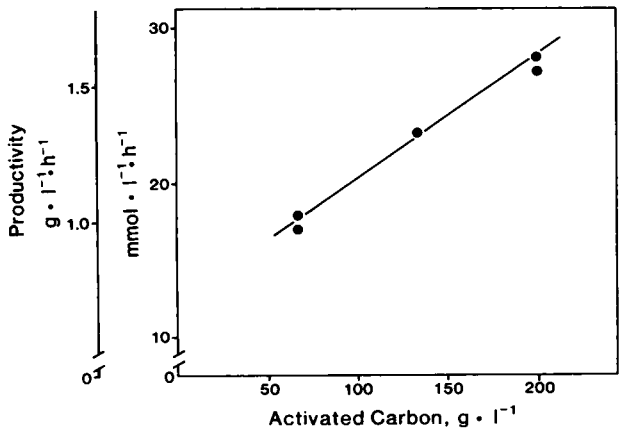


FIG. 7. Ferric iron productivity in the activated-carbon fluidized-bed bioreactor no. 5 (212- to 300-μm-size particles) at various dilution rates. The dilution rate was 0.4/h in these experiments.

TABLE 4. Biomass holdup estimates in the test reactors

| Reactor no. | Total interstitial vol (ml) | Interstitial liquid vol (ml) | Biomass vol in the reactor (ml) | Amt of protein needed to form a monolayer on matrix surface (mg) | No. of monolayers based on observed biomass holdup |
|---|---|---|---|---|---|
| 1 | 29 | 20 | 0.04 | 60 | 0.085 |
| 2 | 25 | 16 | 0.06 | 112 | 0.07 |
| 3 | 23 | 17 | 0.89 | 76 | 1.5 |
| 4 | 17.5 | 10 | 2.7 | 76 | 4.2 |

ning electron microscopy revealed that *T. ferrooxidans* was not established as a tenacious, durable film on the particle surface but was partially removed upon sample preparation (fixation and dehydration) for scanning electron microscopy (unpublished data). It was concluded both from the scanning electron microscopy and from sample fractionation for protein determination that *T. ferrooxidans* cells were washed off during sample manipulations and that the cells remaining on the particle surfaces occurred as individual cells. These cells did not adhere to each other and did not appear to produce extracellular capsular material to facilitate aggregation and adhesion. It was also concluded that a large portion of the actual holdup biomass was associated with surface openings, cavities, and macroporous structures typical in the activated-carbon particles.

**Mineral nutrient effect.** The system reliability was evaluated with the ion-exchange resin packed-bed reactor by switching the inlet from mineral salts solution to acidified tap water while maintaining the same concentration (120 mM) of ferrous sulfate as the energy substrate at $D = 2.5$/h ($D_t = 7.5$/h). The reactor was continuously operated under these conditions for 24 days. During the first 12 days, the productivity in the reactor declined by 16% (Fig. 8). The decline coefficient had a constant value of $-2.1$ mmol/liter per h per day during this period. During the latter 2 weeks of operation, the decline coefficient averaged $-0.16$ mmol/liter per h per day, but the parallel decrease in the productivity was less than 2%.

**Ferric iron precipitation during reactor operation.** All reactors were operated at an initial pH of 1.35. Depending on the relative amount of ferrous iron conversion, pH values as high as 1.5 were measured in effluent samples. Within this pH range of 1.35 to 1.5, the amount of ferric iron precipitation in the reactors was small. For example, in the activated-carbon packed-bed reactor, the total amount of precipitation on the matrix surface amounted to 410 mg during 3 months of continuous operation; i.e., an average of 0.16 mg precipitated per $cm^2$ of activated-carbon matrix. Mineralogically, the precipitation was in the form of jarosite (3). No problems of clogging of interstitial space were observed with the reactors.

## DISCUSSION

The activated-carbon packed-bed bioreactor displayed distinct phases of ferric iron productivity when the dilution rate was varied. These phases are indicated by roman numerals I through IV in Fig. 4 and 5, and they are defined as follows: Phase I, zone of productivity based on loosely and tightly bound biomass; phase II, intermediate zone with peak performance before loosely bound biomass is washed out, resulting in a subsequent decline in ferric iron productivity; phase III, zone of ferric iron productivity based on the activity of tightly bound biomass; and phase IV; zone of declining productivity due to washout of tightly bound biomass.

It should be noted that these phases were differentiated on the basis of the reactor performance and that the description of these phases is essentially based on the performance data of the activated-carbon packed-bed reactor. During the different phases, intermediate sampling of the matrix material for protein determination could not be carried out because of the physical disturbance that it would have caused to the reactor, which would have influenced the reactor performance. Therefore, sampling of the reactors for biomass measurements was carried out only at the termination of each experiment.

When the dilution rate was decreased instead of increased in phases II and III after the loosely bound biomass had washed out, the resulting peak productivity remained lower than that initially achieved with an upward change of the dilution rate. Within phase II, however, a decrease in the dilution rate gradually increased the amount of loosely bound biomass, and thus the productivity values eventually

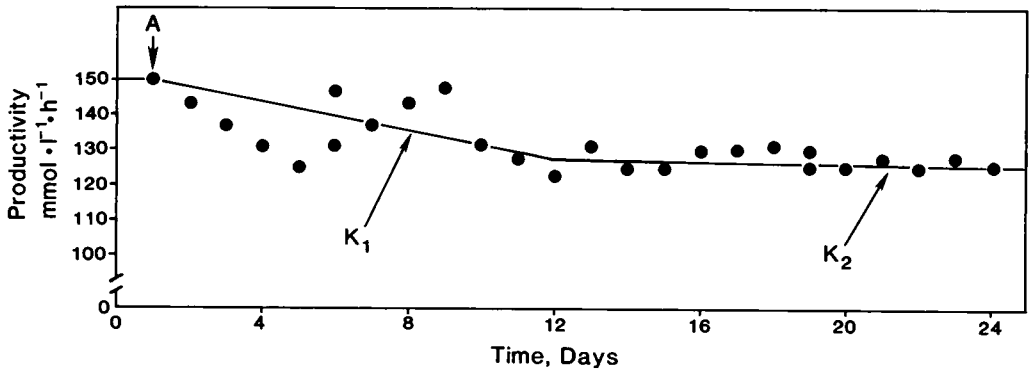


FIG. 8. Ferric iron productivity in the ion-exchange resin packed-bed bioreactor no. 3 when the mineral salts solution was changed to acidified tap water (arrow A). Decline coefficients $K_1$ and $K_2$ are indicated for the 12-day time periods discussed in Results.

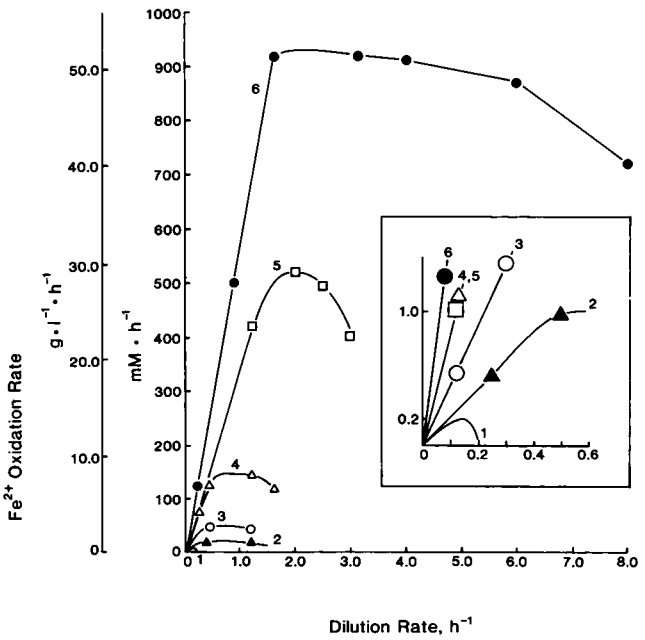


FIG. 9. Ferrous iron oxidation rate at various dilution rates. The data are based on the present study and on previously reported data. 1, Chemostat cultures (data derived from reference 2); 2, fixed-film fiber bioreactor (Grishin and Adamov, in press); 3, glass-bead packed-bed bioreactor (710- to 1,180-μm-size beads); 4, glass-bead packed-bed bioreactor (425- to 600-μm-size beads); 5, ion-exchange resin packed-bed bioreactor; 6, activated-carbon packed-bed bioreactor.

increased after several days of operation (arrow J in Fig. 4). The divisions between the various phases are only approximate. These biomass changes depended on turbulence conditions due to streams of air bubbles and solution in the bioreactors; therefore, these changes were a function of the dilution rate. These phases involving changes in loosely and tightly bound biomass should not be construed as being comparable with the results which differentiate between loosely and tightly bound protein (Table 3). The protein data were based on sample pretreatment by a stripping procedure before the protein assay, and these protein fractions are unrelated to previously discussed biomass changes in phases I through IV. A similar sharp peak in productivity was not observed with the ion-exchange resin and glass-bead packed-bed bioreactors because of the low population density on the carrier matrix.

The real oxidation rates ($R$) in packed-bed reactors were calculated from the respective retention times. The results are shown in Fig. 9. These data indicate a similar degree of effectiveness of the test reactors, with a maximum value of 930 mmol of $Fe^{2+}$ oxidized per liter per h (52 g of $Fe^{2+}$ per liter per h) obtained with the activated-carbon packed-bed reactor. Oxidation rates could be achieved in the test reactor systems which were as high as 1,400 mmol of $Fe^{2+}$ oxidized per liter per h (78 g of $Fe^{2+}$ per l · h) (Table 5).

The data suggested that there was a complex interaction between the amount of biomass, bacterial sorption, physical properties of the carrier matrix, and the hydrodynamic operating conditions. The density of *T. ferrooxidans* sorption was not related to the specific surface area of the carrier matrix. This was evident in the glass-bead packed-bed reactors in which two different bead sizes were used. The total amount of protein attached to the beads was 2.5 and 2.1 μg/cm$^2$ in reactors 1 and 2, respectively (Table 3); the differences between these values were deemed to fall within the experimental and analytical error. The large difference in the biomass sorption on activated-carbon particles in the packed-bed and the fluidized-bed reactors is related to a strong shear effect in the fluidized-bed system. The shear effect was a counterforce which effectively minimized the biofilm formation of *T. ferrooxidans*. It should be noted that scanning electron micrographs of cells on activated-carbon particles revealed a considerable lack of a uniform, homogeneous film (unpublished data). On exposed surfaces, the cells were present as single cells in less than a monolayer formation, and most biomass appeared to be associated with surface fractures, openings, and depressions. The fractionation based on the protein assay of loosely and tightly bound biomass revealed a similar conclusion in that a substantial portion of the biomass could be stripped off from the activated carbon during sample pretreatment. An assumption that a substantial fraction of the total biomass in the packed-bed reactors was present not as a durable biofilm but as microcolonization in interstitial spaces, where its presence was dependent on the hydrodynamic flow conditions, is therefore warranted.

The oxidation quotient values were highest for glass-bead bioreactors and for the fluidized-bed bioreactor (Table 5). These values reflect differences of biomass concentration in the test reactors. These quotients were within the same order of magnitude as was previously reported for chemostat cultures of *T. ferrooxidans* (Table 6). The similarity indicates that there is no major metabolic or kinetic difference in ferrous iron oxidation by freely suspended and attached *T. ferrooxidans* as long as diffusion barriers in the substrate-cells-product complex are similar.

The comparison of the activated-carbon packed-bed bioreactor with other experimental approaches is summarized in Fig. 9 and Table 6. Clearly, the activated-carbon packed-

TABLE 5. Iron oxidation in the test reactors

| Reactor no. | Maximum $Fe^{2+}$ oxidation rate | | $Fe^{2+}$ oxidation quotient[b] | |
|---|---|---|---|---|
| | mmol of $Fe^{2+}$ per liter per h | g of $Fe^{2+}$ per liter per hour | mmol of $Fe^{2+}$ per mg of protein per h | mg of $Fe^{2+}$ per mg of protein per h |
| 1 | 62.5 | 3.5 | 0.25 | 14.0 |
| 2 | 145 | 8.1 | 0.12 | 6.7 |
| 3 | 525 | 29.3 | 0.08 | 4.5 |
| 4 | 930 | 52.0 | 0.02 | 1.1 |
| | 1,400[a] | 78.0[a] | | |
| 5 | 16.5 | 0.9 | 0.14 | 7.9 |

[a] Derived from the initial rates in phase 2 (Fig. 4).
[b] Calculated from rates at the termination of the reactors.

TABLE 6. Comparison of bacterial $Fe^{2+}$ conversion in various experimental approaches

| Experimental technique | Oxidation quotient (mg of $Fe^{2+}$ per mg of protein per h) | Ferric iron productivity (g/liter per h) | Reference |
|---|---|---|---|
| Batch culture | 28.7 | 0.1–0.2 | 15 |
| Chemostat | 50–88 | 0.11–0.2 | 14 |
| | 13–70 | 0.22 | 5 |
| | 68.5 | 0.2 | 2 |
| | 8.5 | 0.12 | 1 |
| Fluidized-bed biofilm reactor | 0.091 | 0.49–1.68 | 6 |
| | | 2.0 | 4 |
| Packed-bed bioreactor | | 1.8 | 13 |
| Rotating biological contactor | | 1.46 | 12 |
| | | 0.7 | 16 |
| Alginate bead column | 0.002 | 0.03 | 7 |
| Fixed-film fiber bioreactor | 5.0 | 1.0–1.2 | In press[a] |
| Bacfox process | | 0.75 | 8 |
| Activated-carbon packed-bed bioreactor | 1.1 | 16 | This study |

[a] S. I. Grishin and E. V. Adamov, Mikrobiologiya, in press.

bed bioreactor exhibited the highest productivity and oxidation rates. Some of the values given in Table 6 for previously reported systems must be viewed as approximate estimates, because the exact data required for calculations were not given in the original references. Where possible, however, maximum oxidation rates given in each reference were used as bases for comparative calculations. By comparison with chemostat data, ferric iron productivity values in the activated-carbon packed-bed bioreactor were about 100 times higher; when compared with packed-bed reactors with high levels of ferric iron precipitates (13), a ninefold increase in the present system is apparent.

The biofilm retained its activity of ferrous sulfate oxidation as acidified tap water was substituted for the mineral salts solution. Thus, a continuous input of nutrient supplementation is not necessary. In the present study, no effort was made to determine the various impurities in the ferrous sulfate and the levels of nutrient ions in the tap water. Any large-scale application of the packed-bed approach to ferric sulfate production would obviously involve numerous impurities and contaminants at minor and trace levels in association with the substrate reagent and process water.

The packed-bed and fluidized-bed bioreactors displayed reliable performance at low pH values during 3 to 4 months of continuous operation. An important feature, particularly with the packed-bed reactor system, was the lack of clogging of interstitial spaces with Fe(III) precipitates. The low pH, which effectively reduced the amount of ferric iron precipitation, made it possible to attain the highest concentration of biomass on a support matrix ever reported for *T. ferrooxidans*. The high level of biomass also resulted in superior reactor performance. Activated carbon was the most suitable carrier matrix for biomass retention in the packed-bed reactor. A combination of the high level of biomass, low pH, negligible ferric iron precipitation, and suitable surface characteristics of activated carbon resulted in the highest level of ferric iron productivity compared with the glass bead and ion-exchange resin systems. The kinetic performance of this approach makes the system attractive for application in wastewater treatment and biological leaching of minerals.

## ACKNOWLEDGMENTS

This work was funded partially by the International Research and Exchange Board.

We thank Laurie Haldeman for typing the manuscript and Peggy Milliman-Wing for administrative support to S.I.G. during his research visit at The Ohio State University.

## LITERATURE CITED

1. **Braddock, J. F., H. V. Luong, and E. J. Brown.** 1984. Growth kinetics of *Thiobacillus ferrooxidans* isolated from arsenic mine drainage. Appl. Environ. Microbiol. **48**:48–55.
2. **Grishin, S. I., E. V. Adamov, and G. I. Karavaiko.** 1983. Intensification of ferrous iron oxidation by *Thiobacillus ferrooxidans*. Mikrobiologiya **52**:322–327.
3. **Grishin, S. I., J. M. Bigham, and O. H. Tuovinen.** 1988. Characterization of jarosite formed upon bacterial oxidation of ferrous sulfate in a packed-bed reactor. Appl. Environ. Microbiol. **54**:3101–3106.
4. **Ishikawa, T., T. Murayama, I. Kawahara, and T. Imaizumi.** 1983. A treatment of acid mine drainage utilizing bacterial oxidation, p. 393–407. *In* G. Rossi and A. E. Torma (ed.), Recent progress in biohydrometallurgy. Associazione Mineraria Sarda, Iglesias, Italy.
5. **Jones, C. A., and D. P. Kelly.** 1983. Growth of *Thiobacillus ferrooxidans* on ferrous iron in chemostat culture: influence of product and substrate inhibition. J. Chem. Technol. Biotechnol. **33B**:241–261.
6. **Karamanev, D. G., and L. N. Nikolov.** 1988. Influence of some physicochemical parameters on bacterial activity of biofilm: ferrous iron oxidation by *Thiobacillus ferrooxidans*. Biotechnol. Bioeng. **31**:295–299.
7. **Lancy, E. D., and O. H. Tuovinen.** 1984. Ferrous ion oxidation by *Thiobacillus ferrooxidans* immobilized in calcium alginate. Appl. Environ. Microbiol. **20**:94–99.
8. **Livesey-Goldblatt, E., T. H. Tunley, and I. F. Nagy.** 1977. Pilot-plant bacterial film oxidation (Bacfox process) of recycled acidified uranium plant ferrous sulphate leach solution, p. 175–190. *In* W. Schwartz (ed.), Conference bacterial leaching. Verlag Chemie, Weinheim, Federal Republic of Germany.
9. **Murayama, T., Y. Konno, T. Sakata, and T. Imaizumi.** 1987. Application of immobilized *Thiobacillus ferrooxidans* for large-scale treatment of acid mine drainage. Methods Enzymol. **136**: 530–540.
10. **Nakamura, K., T. Noike, and J. Matsumoto.** 1986. Effect of operation conditions on biological $Fe^{2+}$ oxidation with rotating biological contactors. Water Res. **20**:73–77.
11. **Nikolov, L., and D. Karamanev.** 1987. Experimental study of the inverse fluidized bed biofilm reactor. Can. J. Chem. Eng. **65**: 214–217.
12. **Nikolov, L., D. Mehochev, and D. Dimitrov.** 1986. Continuous bacterial ferrous iron oxidation by *Thiobacillus ferrooxidans* in rotating biological contactors. Biotechnol. Lett. **8**:707–710.
13. **Nikolov, L., M. Valkova-Valchanova, and D. Mehochev.** 1988. Oxidation of high ferrous iron concentrations by chemolithotrophic *Thiobacillus ferrooxidans* in packed bed bioreactors. J. Biotechnol. **7**:87–94.
14. **Smith, H. R., R. G. Luthy, and A. C. Middleton.** 1988. Microbial ferrous iron oxidation in acidic solution. J. Water Pollut. Control Fed. **60**:518–530.
15. **Tuovinen, O. H., and D. P. Kelly.** 1973. Studies on the growth of *Thiobacillus ferrooxidans*. I. Use of membrane filters and ferrous iron agar to determine viable numbers, and comparison with $^{14}CO_2$ fixation and iron oxidation as measures of growth. Arch. Mikrobiol. **88**:285–298.
16. **Wichlacz, P. L., and R. F. Unz.** 1981. Fixed film biokinetics of ferrous iron oxidation. Biotechnol. Bioeng. Symp. **11**:493–504.